Texture development in Fe-doped alumina ceramics via templated grain growth and their application to carbon nanotube growth

Yasemin Çelik, Ender Suvaci, Alicia Weibel, Alain Peigney, Emmanuel Flahaut

▶ **To cite this version:**

Yasemin Çelik, Ender Suvaci, Alicia Weibel, Alain Peigney, Emmanuel Flahaut. Texture development in Fe-doped alumina ceramics via templated grain growth and their application to carbon nanotube growth. Journal of the European Ceramic Society, 2013, vol. 33, pp. 1093-1100. 10.1016/j.jeurceramsoc.2012.11.013 . hal-00857498

HAL Id: hal-00857498

https://hal.archives-ouvertes.fr/hal-00857498

Submitted on 3 Sep 2013

HAL is a multi-disciplinary open access archive for the deposit and dissemination of scientific research documents, whether they are published or not. The documents may come from teaching and research institutions in France or abroad, or from public or private research centers.

L'archive ouverte pluridisciplinaire **HAL**, est destinée au dépôt et à la diffusion de documents scientifiques de niveau recherche, publiés ou non, émanant des établissements d'enseignement et de recherche français ou étrangers, des laboratoires publics ou privés.

Open Archive Toulouse Archive Ouverte (OATAO)

OATAO is an open access repository that collects the work of Toulouse researchers and makes it freely available over the web where possible.

This is an author-deposited version published in: http://oatao.univ-toulouse.fr/
Eprints ID: 8788

To link to this article: DOI: 10.1016/j.jeurceramsoc.2012.11.013
URL: http://dx.doi.org/10.1016/j.jeurceramsoc.2012.11.013

To cite this version: Çelik, Yasemin and Suvacı, Ender and Weibel, Alicia and Peigney, Alain and Flahaut, Emmanuel *Texture development in Fe-doped alumina ceramics via templated grain growth and their application to carbon nanotube growth.* (2013) Journal of the European Ceramic Society, vol. 33 (n° 6). pp. 1093-1100. ISSN 0955-2219

Any correspondence concerning this service should be sent to the repository administrator: staff-oatao@listes-diff.inp-toulouse.fr

Texture development in Fe-doped alumina ceramics via templated grain growth and their application to carbon nanotube growth

Yasemin Çelik [a], Ender Suvacı [a,*], Alicia Weibel [b], Alain Peigney [b], Emmanuel Flahaut [b,c]

[a] *Department of Materials Science and Engineering, Anadolu University, 26480 Eskisehir, Turkey*
[b] *Université de Toulouse, UPS, INP, Institut Carnot Cirimat, 118 Route de Narbonne, F-31062 Toulouse cedex 9 France*
[c] *CNRS, Institut Carnot Cirimat, F-31062 Toulouse, France*

Abstract

Fe-doped alumina (Fe-Al_2O_3) materials with a controlled microstructure could be designed for some special uses such as a substrate for carbon nanotube growth. In this study, Fe-doped Al_2O_3 ceramics with varying degrees of texture were prepared via Templated Grain Growth method and utilized for carbon nanotube synthesis by Catalytic Chemical Vapor Deposition in order to investigate how α-Al_2O_3 crystal orientation affects carbon nanotube growth in polycrystalline ceramics. The degree of texture increased with the Fe content in the presence of liquid phase. Three kinds of carbon filaments (few-wall carbon nanotubes bundles, individual multi-wall nanotubes and carbon nanofibres) were observed over Fe-doped Al_2O_3 ceramics with varying degrees of texture depending on the surface roughness, crystallographic orientation and the size of the catalyst nanoparticles. While well-textured substrates with a rough surface led to a small amount of randomly oriented carbon nanotube bundles, perpendicularly oriented individual multi-wall nanotubes were obtained over relatively smooth single crystal α-Al_2O_3 platelet surfaces (basal planes) which remained in the matrix without growing.

Keywords: Fe-doped Al_2O_3; Tape casting; Templated grain growth; Carbon nanotubes

1. Introduction

Fe-doped alumina (Fe-Al_2O_3) ceramics exhibit potential as readily available and relatively low cost catalysts for carbon nanotubes (CNTs) synthesis. Peigney et al.[1] have developed a catalytic route for the in situ formation of CNTs over a Fe-Al_2O_3 powder by selective reduction of an alumina–hematite solid solution powder in H_2–CH_4 atmosphere. This simple and scalable technique provides a very homogeneous distribution of CNTs in the CNTs-Fe-Al_2O_3 nanocomposite powder, while avoiding the potentially hazardous effect of handling free CNTs in case of simple mixing with the matrix. Suvaci et al.[2,3] reported successful synthesis of CNTs over polycrystalline Fe-doped Al_2O_3 ceramics by catalytic chemical vapor deposition (CCVD). The authors reported that the size and density of the catalytic nanoparticles showed variations depending on the surface characteristics[2,3]; however, they did not give information about the surface density of these nanoparticles on the polycrystalline surface and did not evaluate whether there is any relationship between crystallographic orientation of grains and CNTs growth. Hongo et al.[4] reported that the single-wall CNTs (SWNTs) yield depends on the crystallographic orientation of sapphire substrate coated with Fe-film and on the film thickness. It is obvious from these studies that there is a correlation between the crystallographic orientation of the single crystal substrate and CNTs growth. Although several single crystals such as quartz and sapphire with a specific crystallographic orientation have been investigated as a substrate for CNTs synthesis,[4–7] polycrystalline ceramics with a textured microstructure have not been used in CNTs growth studies to the best of our knowledge. By texturing Fe-doped Al_2O_3 ceramics, one can evaluate effect of orientation on CNTs growth and hence benefit from the orientation of certain crystallographic planes on the substrate surface for CNTs growth. The crystals of a polycrystalline material can be oriented at certain planes by a variety of techniques such as hot pressing and sinter forging of

* Corresponding author. Tel.: +90 222 321 3550/6359; fax: +90 222 323 9501.
E-mail address: esuvaci@anadolu.edu.tr (E. Suvacı).

http://dx.doi.org/10.1016/j.jeurceramsoc.2012.11.013

systems containing oriented whisker-, fibre-, or platelet-shaped particles.[8–10] Templated Grain Growth (TGG) is another widely utilized method for the production of textured ceramics.[11] In TGG, a small number of large anisometric template particles are aligned in a fine powder matrix during tape casting, slip casting, extrusion or uniaxial pressing. After densification, these larger anisometric grains grow and consume the matrix grains to yield ceramics with textured grains and high degrees of crystallographic orientation. Consequently, the objective of this study was to investigate how to tailor microstructure in Fe-doped Al_2O_3 ceramics via TGG method in order to achieve a controlled degree of texture by controlling the amount of Fe and/or sintering conditions, and then to investigate the possible use of these ceramics as substrates for the catalytic growth of CNTs. It was also aimed to evaluate role of crystallographic orientation of Fe-doped α-Al_2O_3 crystals on CNTs growth.

2. Experimental procedure

2.1. Texture formation

1%, 2%, 5% and 10 cat.% Fe-doped Al_2O_3 powders ($Al_{2(1-x)}Fe_{2x}O_3$ ($x \leq 0.1$)), later used as matrix material for textured substrate fabrication, were synthesized by combustion synthesis method as described by Cordier et al.[12] In this process, the required proportion of aluminum nitrate nonahydrate ($Al(NO_3)_3{\cdot}9H_2O$, Merck, extra pure) and iron nitrate nonahydrate ($Fe(NO_3)_3{\cdot}9H_2O$, Merck, GR for analysis) were dissolved in distilled water in a Pyrex® beaker. A mixture of citric acid and urea (75% citric acid and 25% urea) was used as fuel, in a quantity equal to twice the stoichiometric ratio.[12] The required amount of citric acid and urea were dissolved in distilled water and then added into the nitrate solution. The solution was stirred at 600 rpm and ca. 120 °C for 1 h. The Pyrex® beaker was then placed in a preheated furnace, at 550 °C, and kept there for at least 20 min. The as-synthesized amorphous powder was subjected to two-stage calcination process: it was first heated at 5 °C/min up to 600 °C, 1.5 h of dwell time in order to remove the residual carbon and then at 15 °C/min up to 1100 °C, 20 min of dwell time to obtain the α-phase. After calcination, the powders were attrition milled at 250 rpm for 4 h in distilled water by using yttria-stabilized ZrO_2 balls, 3 mm in diameter.

Fe-doped Al_2O_3 ceramic substrates were prepared by tape casting. The matrix consisted of the α-$Al_{2(1-x)}Fe_{2x}O_3$ powder with a specific surface area of $\sim$33 m^2/g. 5 vol% α-Al_2O_3 platelets (Pyrofine Platelets, Elf-Atochem, Pierre-Benite, France) of 20 ± 5 μm in diameter and 2.0 μm thickness were added to the matrix as templates. CaO and SiO_2 were used as high temperature glass formers at a ratio of 1.3:1 in an amount of 0, 1 or 5 vol% of the matrix powder. Tape casting slurry consisted of an azeotropic mixture of methylethylketone (MEK, 66 vol%) and ethanol (EtOH, 34 vol%) as solvent, sodiumtripolyphosphate (STPP) as dispersant, polyvinylbutyral (PVB Butvar 76) as binder, and polyethylene glycol (PEG 3000, Fluka, Steinheim, Switzerland) and dibutylphthalate (DBP) as plasticizers.

A suspension with 39 vol% solids loading was prepared by dispersing α-$Al_{2(1-x)}Fe_{2x}O_3$ powder in the azeotropic mixture of MEK and EtOH with 8 vol% STPP by ball milling for 4 h using yittria-stabilized ZrO_2 balls, 3 mm in diameter. PEG (11 vol%) and DBP (4 vol%) were added to the suspension and again ball milled for 2 h. Then, PVB (23 vol%) was added and the suspension was again ball milled for additional 15 h. After ball milling, α-Al_2O_3 platelets were added to the slurry and mixed with a magnetic stirrer for 2 h. The prepared slurry was tape casted on a glass plate at a blade height of 400 μm at a 30 cm/s casting speed. After drying at ambient conditions for 30 min, the tape was cut and laminated at 45 MPa and 70 °C for 10 min. Laminated tapes were heat treated for removing organics by heating the samples to 450 °C at a rate of 1 °C/min and holding them at this temperature for 2 h. Unless otherwise noted, the samples were sintered at 1600 °C for 2 h in air with heating and cooling rates of 10 °C/min. The notation for samples is *x*FeyLP, where *x* is the cationic percent of Fe in the α-$Al_{2(1-x)}Fe_{2x}O_3$ powder and y is the volume fraction of liquid phase formers (LP), $CaO + SiO_2$, in the initial powder mixture. The volume fraction of α-Al_2O_3 platelets (i.e., PL) was 5 vol% for all samples unless otherwise indicated.

Microstructure development of sintered samples was examined using scanning electron microscope (SEM, Zeiss EVO 50). The SEM analyses were performed on polished and thermally etched cross-section surfaces. The dimensions and aspect ratios of anisotropic grains were directly measured from micrographs (at least 24 measurements) and averaged. Crystallographic texture development in the samples was characterized by an X-ray diffractometer (XRD, Rigaku Rint 2200, Tokyo, Japan) with Cu$K\alpha_1$ radiation. Texture fraction of the samples was determined by Lotgering Factor, which is an X-ray based semi-quantitative characterization method.[13]

2.2. Carbon nanotube growth

The sintered samples were then placed in alumina boats in the middle of a CCVD chamber and reduced in H_2–CH_4 gas mixture (82 mol% H_2 as reducing gas and 18 mol% CH_4 as carbon source) at 1000 °C with a heating and cooling rate of 5°/min. No dwell time was applied.[1,14] After CCVD, the samples were characterized by field-emission-gun scanning electron microscope (FEG-SEM, Jeol JSM 6700F at TEMSCAN, Universite Paul-Sabatier).

3. Results and discussion

3.1. Texture development

Texture development was investigated as a function of Fe content and liquid phase former amount by keeping α-Al_2O_3 template amount, sintering temperature and time constant. The SEM micrographs in Fig. 1 show the effect of Fe-content on the microstructure development of 5 vol% template (α-Al_2O_3)-containing alumina samples solid-state sintered at 1600 °C for 2 h. No texture could be achieved for the solid-state sintered Fe-doped Al_2O_3 samples at that temperature, whatever their Fe content. Neither matrix nor platelet grains exhibited significant grain growth in the samples with low Fe content (i.e., 1Fe0LP

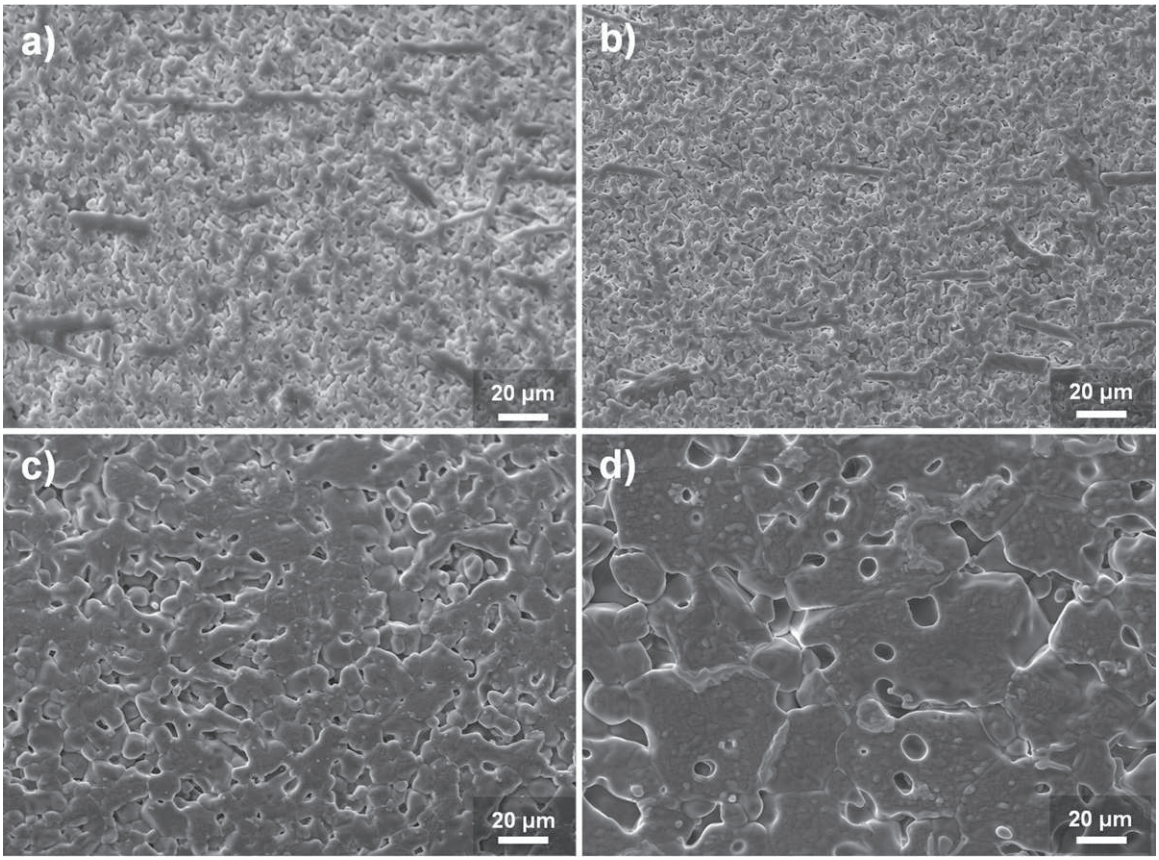

Fig. 1. SEM micrographs of (a) 1Fe0LP, (b) 2Fe0LP, (c) 5Fe0LP and (d) 10Fe0LP samples sintered at 1600 °C for 2 h.

and 2Fe0LP) due to limited degree of densification, although the samples were sintered at a relatively high temperature (Fig. 1(a) and (b)). This retardation in densification could be attributed to the negative effect of platelets on the packing of the matrix particles. Özer et al.[15] and Belmonte et al.[16] investigated the sintering behavior of alumina powder compacts containing alumina platelet particles and showed that α-Al_2O_3 platelet particles hindered densification. Carisey et al.[17] also suggested that platelets constrained densification in solid-state sintered Al_2O_3. While 1 and 2 cat.% Fe-doping could not suppress the negative effect of platelets on densification, it was observed that increasing the Fe content to 5 and especially to 10 cat.% influenced the microstructure development of platelet-containing alumina significantly (Fig. 1(c) and (d)). In 5Fe0LP sample, matrix grains also grew to some extent besides the platelets, leading to large pores in the microstructure (Fig. 1(c)). Increasing the Fe content further to 10 cat.% (10Fe0LP) resulted in exaggerated grain growth, where it is not easy to distinguish whether these abnormally and isotropically grown grains formed from the matrix or from the platelets (Fig. 1(d)). Both inside and between these grains, a high amount of large pores were formed. It is obvious from the micrographs that certain amount of Fe-doping (i.e., ≥5 cat.%) improves the sintering behavior of platelet-containing Al_2O_3. Calculations based on sintering equations showed that the diffusion coefficients increase with increasing Fe content; consequently, the sintering rate of Fe-doped Al_2O_3 increases with increasing total Fe amount.[18] It was also reported that addition of Fe_2O_3 into Al_2O_3 over a certain amount can promote anisotropic and exaggerated grain growth at high temperatures such as 1650 °C.[19] This arises from reduction of some of the Fe^{3+} to Fe^{2+} leading to creation of oxygen vacancies or aluminum interstitials which increase grain boundary diffusion and from segregation of a significant amount of Fe^{2+} to grain boundaries resulting in an exaggerated grain growth.[19] At 1450–1500 °C in air, iron is primarily in the trivalent state, and only 2% of the total Fe^{3+} is reduced.[20] The solubility of Fe^{2+} in Al_2O_3 is 0.7–1.9% at 1450 °C.[19,21] The reduction of Fe^{3+} to Fe^{2+} over the solubility limit results in segregation of free iron oxide at grain boundaries forming $FeAl_2O_4$ phase and causes rapid growth and uncontrolled microstructural development.[19,22] In the present study, the increasing grain growth with increasing Fe^{3+} doping could be attributed to formation of higher amount of Fe^{2+} due to reduction of Fe^{3+} cations. For the samples with lower iron content (e.g., 1 and 2 cat.%), the amount of reduced Fe^{3+} may not be sufficient to promote enhanced grain growth. For the 5Fe0LP sample, the amount of Fe^{2+} formed by the reduction of Fe^{3+} is higher than that of the 1Fe0LP and 2Fe0LP; however the amount of Fe^{2+} is still below the solubility limit; therefore, the enhanced grain growth could be explained by the mechanism based on the creation of oxygen vacancies as suggested by Tartaj and Messing.[19] As the iron content increases to 10 cat.%, higher amount of Fe^{3+} is reduced (over the solubility limit) and this may cause the segregation at grain boundaries resulting to an exaggerated grain growth. However, a textured

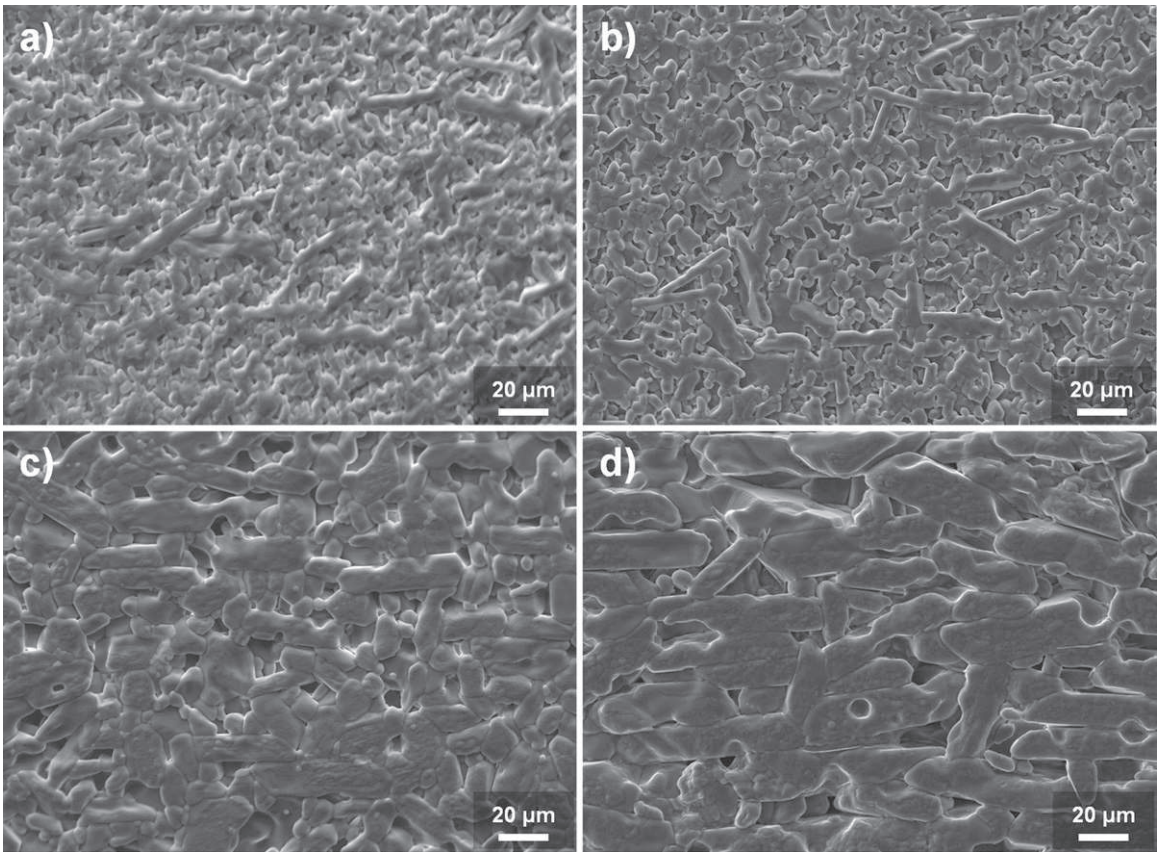

Fig. 2. SEM micrographs of (a) 1Fe1LP, (b) 2Fe1LP, (c) 5Fe1LP and (d) 10Fe1LP samples sintered at 1600 °C for 2 h.

microstructure could not be achieved for the solid state sintered Fe-doped Al_2O_3 samples due to uncontrolled microstructure development, although the negative effect of platelet particles on densification of Al_2O_3 was suppressed by certain amount of Fe-doping.

Therefore, the samples were also liquid-phase sintered with different liquid phase amounts to be able to control the microstructure, based on the information from the previous studies where it was shown that liquid phase sintering reduces constrained densification caused by the template particles and accelerates grain growth[23–25] and where it was reported that the addition of CaO and SiO_2 creates favorable kinetic conditions for anisotropic grain growth during sintering.[24,26]

Fig. 2(a)–(d) show the SEM micrographs of liquid phased sintered 1Fe1LP, 2Fe1LP, 5Fe1LP and 10Fe1LP samples, respectively. The liquid phase regulated the microstructure and promoted anisotropic growth of the platelets in the Fe-doped Al_2O_3 samples, prominently as from 5 cat.% Fe doping. The degree of texture increased with increasing Fe content at the presence of liquid phase, due to existence of the strong influence of certain amount of Fe-doping on the sintering kinetics of alumina and the effect of liquid phase on anisotropic growth of the template particles together in the system. The texture formation becomes apparent with the 5% Fe doping (Fig. 2(c)) and the 10Fe1LP system shows the highest morphological texture among the other 1% LP former containing samples (Fig. 2(d)). The average aspect ratio of the anisotropic grains in this sample is ~4.1 with an average diameter of 59 μm and thickness of 14 μm. Besides the well oriented template grains along the tape casting direction, some misoriented templates are also present leading to the formation of large pores in the microstructure.

Fig. 3 shows the effect of 5% LP former addition on the texture development of 5 and 10% Fe-doped samples, which were also sintered at 1600 °C for 2 h. The increased liquid phase amount led to more faceted template grains with a higher average aspect ratio in these samples.[26] The aspect ratio of 10Fe5LP sample was ~6.1. The average diameter of anisotropic grains in this sample was 57 μm and the average thickness was 9 μm. Besides the aligned grains in the tape casting direction, some coarse matrix grains and misaligned anisotropic grains also remained. These grains hindered densification and subsequently the radial growth of aligned templates. Consequently, large pores between the template grains were formed, preventing to achieve a higher degree of texture. Seabaugh et al.[26] reported that liquid phase dramatically affects densification and the faceting of grains and degree of grain faceting increases as the amount of liquid phase increases.

The XRD analyses of the top surfaces of 10Fe0LP, 10Fe1LP and 10Fe5LP samples are shown in Fig. 4. The XRD patterns revealed crystallographic texture in the liquid phase containing Fe-doped Al_2O_3 samples in agreement with the morphological texture, observed in SEM images. An increase in the ratio of basal plane peak intensities (0 0 0 6) and (0 0 0 1 2) relative to the peak with the highest intensity in the non-template containing sample (1 1 $\bar{2}$ 3) was observed. The intensity ratios of the (0 0 0 6) to (1 1 $\bar{2}$ 3) peaks were 0.05, 0.31, 1.59 and 0.81 for the

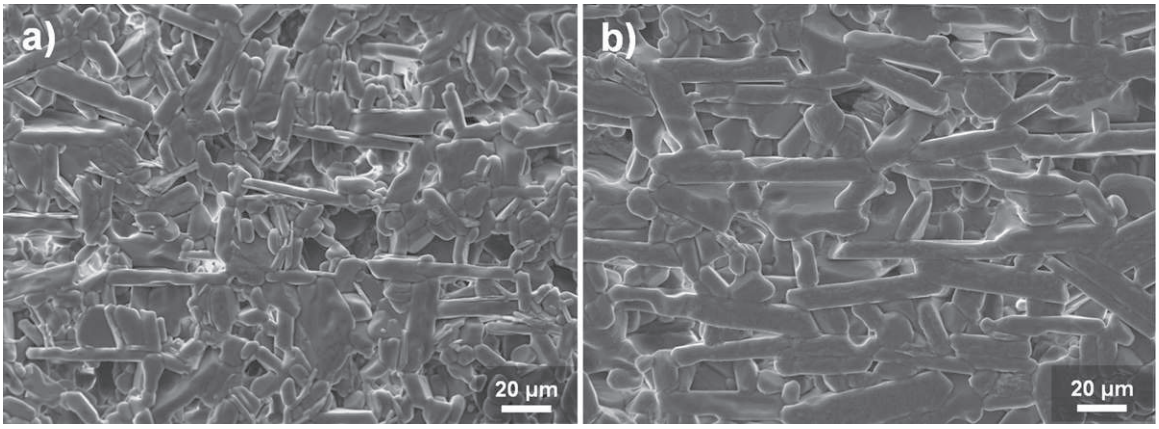

Fig. 3. SEM micrographs of (a) 5Fe5LP and (b) 10Fe5LP samples sintered at 1600 °C for 2 h.

10% Fe-doped sample without any template and liquid phase formers, 10Fe0LP, 10Fe1LP and 10Fe5LP samples, respectively. The highest texture fraction revealed by Lotgering factor calculations was ca. 0.33 for 10Fe1LP system. The texture degree of these Fe-doped Al_2O_3 ceramics could be improved by controlling the orientation of platelet particles in the matrix powder, liquid phase content, platelets amount, rheology of tape casting slurry, sintering temperature and time. However, the texture level obtained in this study was sufficient to investigate how a textured ceramic substrate could affect CNTs growth by CCVD.

3.2. Carbon nanotubes growth over textured Fe-doped Al_2O_3

Fig. 5 shows the schematic representation of texture development in Fe-doped Al_2O_3 by TGG and the proposed CNTs growth over this textured ceramic substrate by CCVD. 5 vol% α-Al_2O_3 platelet shaped templates were oriented in fine Fe-doped Al_2O_3 matrix by tape casting with their basal planes parallel to the substrate surface. By a subsequent heat treatment, these templates grew at the expense of the matrix. Since they maintained their original position during grain growth, the substrate surface was covered by the basal planes of the templates at the end of TGG process. The CNTs growth by CCVD was performed on this top basal plane oriented surface of the substrate. According to our hypothesis, when the textured substrate is subjected to CCVD, homogeneously distributed substitutional Fe^{3+} cations are first reduced to metallic Fe atoms and then coalesce into clusters and later catalytic nanoparticles by selective reduction. We now investigate the CNTs growth by CCVD over these substrates.

Fig. 6 shows the SEM micrographs of the top surface of CCVD-subjected 10Fe1LP and 10Fe5LP samples, which show

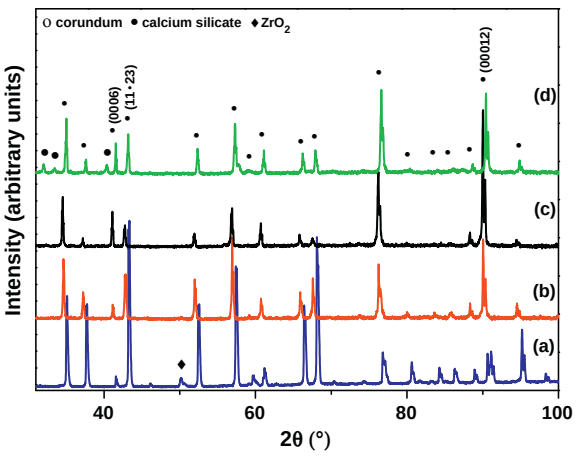

Fig. 4. XRD patterns of the (a) 10 cat.% Fe without any platelets and LP (b) 10Fe0LP, (c) 10Fe1LP and (d) 10Fe5LP samples sintered at 1600 °C for 2 h. (0 0 0 6) and (0 0 0 1 2) indicate the Miller indices for basal planes of α-Al_2O_3 platelets.

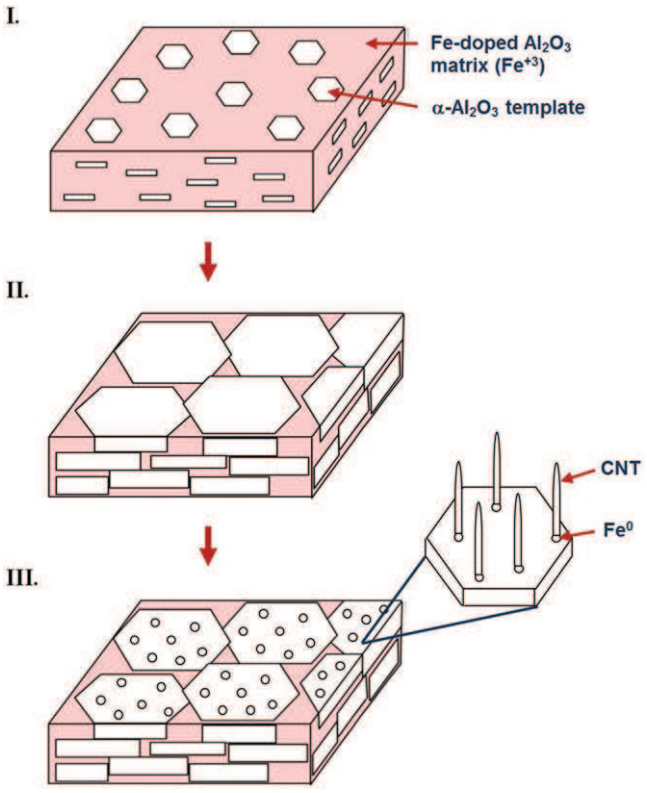

Fig. 5. Schematic representation of textured Fe-doped Al_2O_3 production by TGG method and CNTs growth over these ceramics by CCVD (I. Tape casting, II. Sintering, and III. CCVD steps).

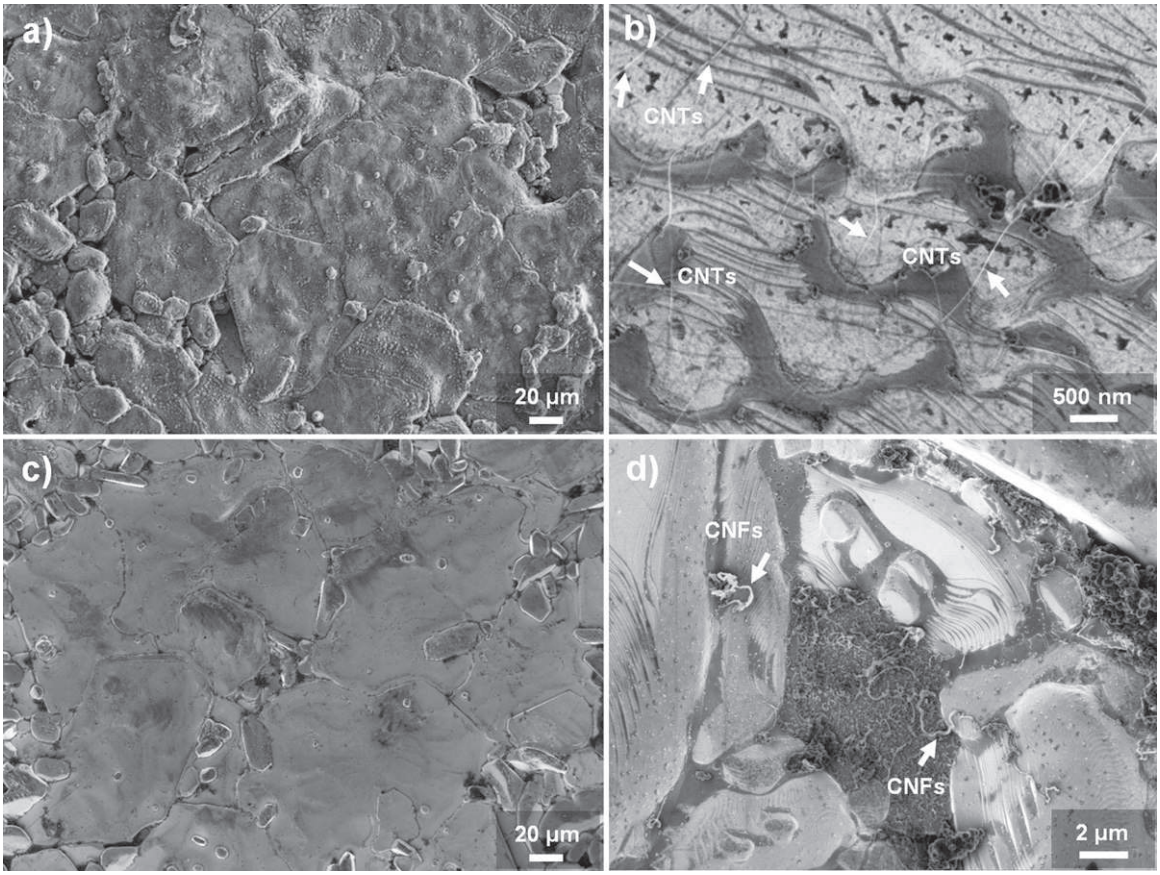

Fig. 6. SEM micrographs of 10Fe1LP (a, b) and 10Fe5LP (c, d) after CCVD process. (b) and (d) are higher magnification images of the corresponding samples. White arrows indicate carbon nanotubes (CNTs) and carbon nanofibers (CNFs) in (b) and (d), respectively.

a relatively higher degree of texture compared to others. On the contrary of our hypothesis, these substrates led to small amounts of randomly oriented CNTs. Fig. 6(a) and (b) show a general view of the surface morphology of 10Fe1LP sample after CCVD and a higher magnification image of this sample, showing both long and flexible interconnected filaments, characteristic of bundles of few-wall CNTs (indicated by white arrows) and the absence of any carbon nanofibre, respectively. This sample presented a bimodal microstructure with relatively small matrix grains and much larger template grains which were grown by consuming the matrix grains forming a quite rough surface topography (Fig. 6(a)). This surface roughness could be responsible for the small amount of randomly oriented CNTs growth since it may have affected the density and size of the catalytic nanoparticles (Fig. 6(b)). Suvaci et al.[2,3] observed randomly oriented CNTs bundles over polycrystalline Fe-doped Al_2O_3 ceramics. The authors reported that the CNTs yield was relatively low with respect to the total number of catalytic nanoparticles and they suggested that the variation in catalytic nanoparticle size on polycrystalline substrates may arise from the variation of cluster formation kinetics depending on the surface morphology and crystallographic orientation of the grains.[2,3] Cao et al.[27] reported dense, randomly oriented bamboo-like multi walled CNTs with different outer diameters over metallic film-coated rough polycrystalline Al_2O_3, where catalytic nanoparticles with varying sizes and shapes were formed since each nanoparticle was formed on its unique position. The surface of 10Fe5LP looked much smoother than that of 10Fe1LP, although it could be still defined as rough (Fig. 6(c)). This is most probably due to an increased liquid phase amount which promoted the growth of more faceted template grains. Very few CNTs were formed on this substrate, while a relatively higher amount of carbon nanofibers and other non-tubular carbonaceous species were observed, especially on the phase which comes from the liquid phase and located at grain boundaries (Fig. 6(d)). It should be noted here that some non-tubular carbon forms like carbon nanofibers were also observed even in the samples without any liquid phase former addition. This may have arised from the impurities (like SiO_2) in the platelets which could have formed a liquid phase during sintering. Another reason could be the secondary phase segregated at grain boundaries. Probably, a high amount of Fe species in the grain boundary phase could have caused larger Fe nanoparticles upon reduction and thus carbon nanofibers instead of CNTs.

Although oriented CNTs could not be grown over well textured substrates, some interesting results were observed during this study. Fig. 7 shows the FEG-SEM micrographs of a 5 cat.% Fe-doped Al_2O_3 sample, containing 5 vol% liquid phase formers (CaO and SiO_2) and 5 vol% 20 μm α-Al_2O_3 platelets,

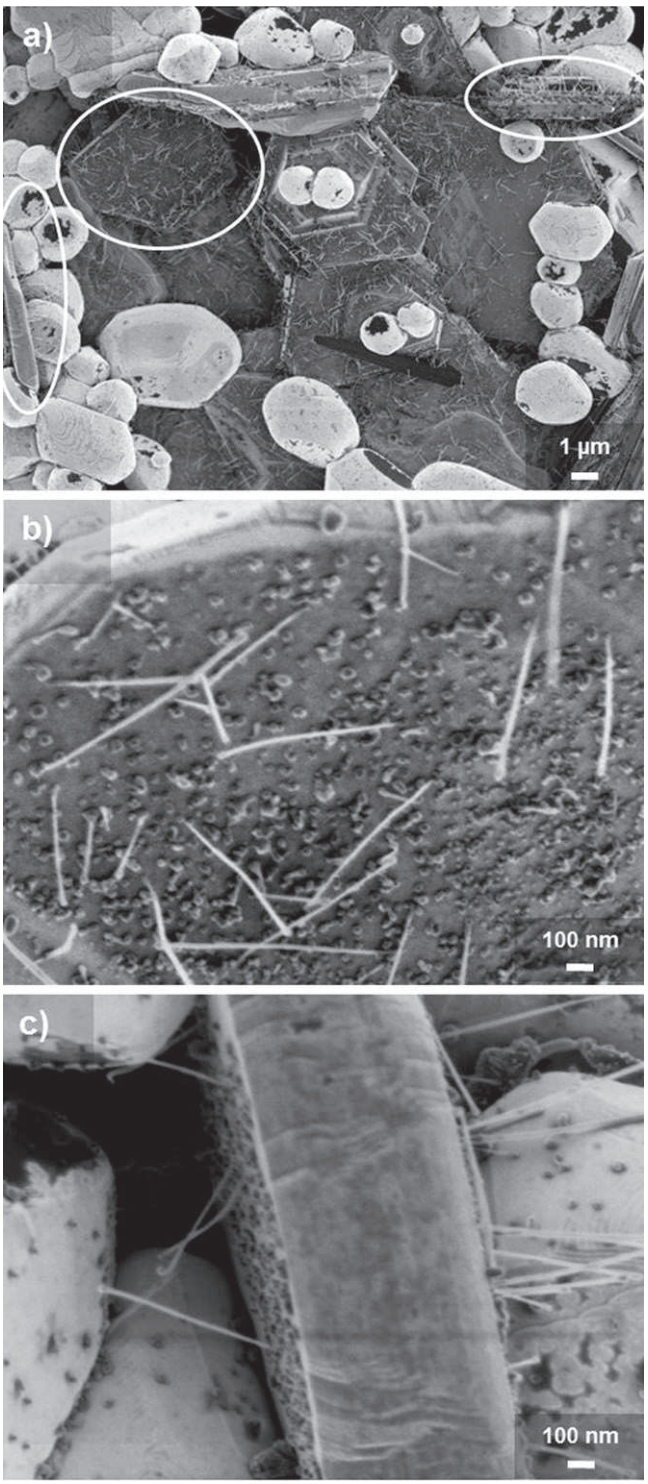

Fig. 7. (a) FEG-SEM micrograph of the vertically aligned CNT growth over basal planes of α-Al_2O_3 platelets in 5 cat.% Fe-doped Al_2O_3 sample with 5 vol% liquid phase former content sintered at 1400 °C for 2 h. (b, c) Higher magnification images of CNTs over α-Al_2O_3 platelets.

after CCVD. The sample was sintered at a lower temperature (1400 °C) for 2 h. The SEM micrograph in Fig. 7(a) reveals that α-Al_2O_3 platelets were distributed randomly and inhomogeneously in the matrix and they could not grow during sintering, while matrix grains grew to some extent. However, interestingly, short and very rigid CNTs were grown perpendicularly to the basal planes of these α-Al_2O_3 platelets, as shown in Fig. 7(b) and (c). These are probably large diameter individual multi-wall CNTs (MWNTs) rather than bundles of few-wall CNTs. It was also observed that a high amount of Fe nanoparticles, only a small part of which catalyzed CNTs growth, were formed over the basal planes of the platelets. It is proposed that some Fe^{3+} cations diffused into the platelets during sintering and were reduced into the Fe^0 during CCVD preferentially at the basal planes of the platelets. Hongo et al.[4] reported that SWNTs yield depended on the crystallographic orientation of sapphire substrate coated with Fe-film and on the film thickness. The authors explained this result with different diffusion constants of Fe on the sapphire surfaces or affinity between Fe and the substrate surface.[4] In contrast to the textured substrates, the surface of the α-Al_2O_3 platelets is quite smooth. This obviously supports the fact that the surface roughness of the substrate and crystallographic orientation of grains play a critical role on the size, location and orientation of catalytic nanoparticles and subsequently on orientation of CNTs.

These results indicated that three kinds of carbon filaments (few-wall CNTs bundles, individual MWNTs and CNFs) were grown over Fe-doped Al_2O_3 substrates with varying degrees of texture. While rough textured substrate surface resulted in randomly oriented long and flexible CNTs bundles, perpendicularly oriented individual MWNTs were observed over relatively smooth single crystal α-Al_2O_3 platelet surfaces (basal planes) in a non-textured Fe-doped Al_2O_3 sample. CNFs and other forms of non-tubular carbonaceous forms were observed at grain boundaries where segregated secondary phase and the liquid phase located and affected the catalytic Fe nanoparticle size.

4. Conclusions

Fe-doped Al_2O_3 ceramics with a textured microstructure were produced by templated grain growth method. Fe-doping into Al_2O_3 helped sintering; however, exaggerated grain growth occurred at high amount of Fe addition (i.e., ∼10 cat.%) at 1600 °C. Introducing CaO-SiO_2 as liquid phase formers into the system enhanced densification and liquid-phase sintering promoted anisotropic grain growth in those samples. The degree of texture increased with the Fe content in the presence of liquid phase. 1 vol% liquid phase former-added 10 cat.% Fe-doped Al_2O_3 sample showed the highest degree of texture, while a very limited template growth occurred in 1 and 2 cat.% Fe-doped samples. The Fe-doped Al_2O_3 ceramics with varying degrees of texture were subjected to CCVD and three kinds of carbon filaments (few-wall CNTs bundles, individual MWNTs and CNFs) were grown over these substrates depending on the surface roughness, the size of the catalyst nanoparticles and the grain boundary phase. Well textured substrates led to randomly oriented few amount of CNTs bundles. However, on a substrate where no template growth occurred due to random and inhomogeneous distribution of α-Al_2O_3 platelets in the Fe-doped Al_2O_3 matrix and insufficient sintering temperature, individual MWNTs were grown

perpendicular to the basal planes of single crystal α-Al_2O_3 platelets.

Acknowledgements

The financial support for this study by The Scientific and Technological Research Council of Turkey (TUBITAK) and Centre National de la Recherche Scientifique (CNRS) under the contract number 106M543 is gratefully acknowledged. One of the authors, E. Suvaci, thanks to Turkish Academy of Sciences (TUBA) for financial support through Outstanding Young Investigator Award (GEBIP) Programme. Anadolu University Scientific Research Projects Commission (under the project number of 050262) is also gratefully acknowledged for their support to this study.

References

1. Peigney A, Laurent Ch, Dobigeon F, Rousset A. Carbon nanotubes grown in-situ by a novel catalytic method. *J Mater Res* 1997;**12**:613–5.
2. Suvacı E, Çelik Y, Weibel A, Peigney A, Flahaut E. Organized growth of carbon nanotubes on Fe-doped alumina ceramic substrates. *Carbon* 2012;**50**:3092–5.
3. Bozkaya Y. Karbon Nanotüp Sentezinde Kullanılmak Üzere Fe-Katkılı Al_2O_3 Seramik Tozlarının ve Altlıkların Üretimi. *M.Sc. Thesis*. Turkey: Anadolu University; 2008.
4. Hongo H, Yudasaka M, Ichihashi T, Nihey F, Iijima S. Chemical vapor deposition of single-wall carbon nanotubes on iron-film-coated sapphire substrates. *Chem Phys Lett* 2002;**361**:349–54.
5. Ago H, Nakamura K, Ikeda K, Uehara N, Ishigami N, Tsuji M. Aligned growth of isolated single-walled carbon nanotubes programmed by atomic arrangement of substrate surface. *Chem Phys Lett* 2005;**408**:433–8.
6. Han S, Liu X, Zhou CJ. Template-free directional growth of single-walled carbon nanotubes on a- and r-plane sapphire. *Am Chem Soc* 2005;**127**(15):5294–5.
7. Ismach A, Segev L, Wachtel E, Joselevich E. Atomic-step-templated formation of single wall carbon nanotube patterns. *Angew Chem Int Ed* 2004;**43**(45):6140–3.
8. Kimura T, Yahimoto T, Iida N, Fujita Y, Yamaguchi T. Mechanism of grain orientation during hot-pressing of bismuth titanate. *J Am Ceram Soc* 1989;**72**:85–9.
9. Ma Y, Bowman KJ. Texture in hot-pressed or forged alumina. *J Am Ceram Soc* 1991;**74**:2941–4.
10. Watanabe H, Kimura T, Yamaguchi T. Sintering of platelike bismuth titanate powder compacts with preferred orientation. *J Am Ceram Soc* 1991;**74**:139–47.
11. Seabaugh MM, Hong SH, Messing GL. Processing of textured ceramics by templated grain growth. In: Tomsia AP, Glaeser A, editors. *Ceramic microstructure: control at the atomic level*. New York: Plenum; 1998. p. 303–10.
12. Cordier A, Peigney A, De Grave E, Flahaut E, Laurent C. Synthesis of the metastable α-$A_{l1.8}Fe_{0.2}O_3$ solid solution from precursors prepared by combustion. *J Eur Ceram Soc* 2006;**26**:3099–111.
13. Lotgering FK. Topotactical reactions with ferrimagnetic oxides having hexagonal crystal structures-I. *J Inorg Nucl Chem* 1959;**9**: 113–23.
14. Flahaut E, Bacsa R, Peigney A, Laurent Ch. Gram-scale CCVD synthesis of double walled carbon nanotubes. *Chem Commun* 2003;**12**: 1442–3.
15. Ozer IO, Karademir B, Dogan A, Suvaci E, Missiaen JM, Bouvard D, et al. Anisotropic shrinkage in solid state sintering of alumina ceramics with oriented platelets. *J Am Ceram Soc* 2006;**89**:1972–6.
16. Belmonte M, Moreno R, Moya JS, Miranzo P. Obtention of highly dispersed platelet reinforced Al_2O_3 composites. *J Mater Sci* 1994;**29**: 179–83.
17. Carisey T, Laugier-Werth A, Brandon DG. Control of texture in Al_2O_3 by gel-casting. *J Eur Ceram Soc* 1995;**15**:1–8.
18. Rao WR, Cutler IB. Effect of iron oxide on the sintering kinetics of Al_2O_3. *J Am Ceram Soc* 1973;**56**:588–93.
19. Tartaj J, Messing GL. Anisotropic grain growth in α-Fe_2O_3-doped alumina. *J Eur Ceram Soc* 1997;**17**:719–25.
20. Ikuma Y, Gordon RS. Effect of doping simultaneously with iron and titanium on the diffusional creep of polycrystalline alumina. *J Am Ceram Soc* 1983;**66**:139–47.
21. Muan A. On the stability of the phase Fe_2O_3-Al_2O_3. *Am J Sci* 1958;**256**:413–22.
22. Tartaj P, Tartaj J. Microstructural evolution of iron-oxide-doped alumina nanoparticles synthesized from microemulsions. *Chem Mater* 2002;**14**:536–41.
23. Seabaugh MM. Texture development in liquid phase sintered alpha alumina via anisotropic template growth. *Ph.D. Dissertation*. University Park: The Pennsylvania State University; 1998.
24. Seabaugh MM, Messing GL, Brahmaroutu B. Anisotropic template growth in textured alumina. In: You HI, Joong S, editors. *Interfaces '98*. London: Institute of Materials; 2000.
25. Suvaci E, Seabaugh MM, Messing GL. Reaction-based processing of textured alumina by templated grain growth. *J Eur Ceram Soc* 1999;**19**:2465–74.
26. Seabaugh MM, Kerscht I, Messing GL. Texture development by templated grain growth in liquid-phase sintered alpha-alumina. *J Am Ceram Soc* 1997;**80**:1181–8.
27. Cao PJ, Zhu DL, Liu WJ, Ma XC. The effect of substrate morphology on the diameter distribution of carbon nanotubes grown on silica and ceramic substrates. *Mater Lett* 2007;**61**(8–9):1899–903.